

Supporting Information

I. Experimental Section

Catalyst synthesis. All perovskite oxides in this study were synthesized by a combined ethylenediaminetetraacetic acid-citric acid (EDTA-CA) complexing sol-gel method. Taking the synthesis of $\text{La}_{0.4}\text{Sr}_{0.4}\text{Ti}_{0.9}\text{Ni}_{0.1}\text{O}_{3-\delta}$ (LSTN) as an example, tetrabutyl titanate ($\text{C}_{16}\text{H}_{36}\text{O}_4\text{Ti}$) and CA at a molar ratio of 1:5 were mixed in deionized water at 80°C under vigorous stirring until the solution was clear, and then stoichiometric amounts of $\text{La}(\text{NO}_3)_3 \cdot 6\text{H}_2\text{O}$, $\text{Sr}(\text{NO}_3)_2$ and $\text{Ni}(\text{NO}_3)_2 \cdot 6\text{H}_2\text{O}$ (both analytical grade, Sinopharm Chemical Reagent Co., Ltd.) were then added to the above solution. EDTA and CA were added sequentially as complexing agents at a mole ratio of 1:1:2 for total metal ions/EDTA/CA, followed by $\text{NH}_3 \cdot \text{H}_2\text{O}$ which was poured into the resulting solution to adjust the pH to 6-7. A transparent gel was obtained by heating at 90°C under stirring. The gel was then heated in the oven at 250°C for 5 h in air to form a solid precursor. Finally, the solid precursor was calcined at 1000°C for 10 h in air to form LSTN powder. The other perovskite oxides used in this study, namely, $\text{La}_{0.4}\text{Sr}_{0.4}\text{Ti}_{0.9}\text{O}_{3-\delta}$ (LST), $\text{La}_{0.4}\text{Sr}_{0.4}\text{Ti}_{0.9}\text{Co}_{0.1}\text{O}_{3-\delta}$ (LSTC), $\text{La}_{0.4}\text{Sr}_{0.4}\text{Ti}_{0.9}\text{Fe}_{0.1}\text{O}_{3-\delta}$ (LSTF), $\text{La}_{0.4}\text{Sr}_{0.4}\text{Ti}_{0.9}\text{Ni}_{0.075}\text{Fe}_{0.025}\text{O}_{3-\delta}$ (LSTNF), $\text{La}_{0.4}\text{Sr}_{0.4}\text{Ti}_{0.9}\text{Ni}_{0.05}\text{Co}_{0.05}\text{O}_{3-\delta}$ (LSTNC), $\text{La}_{0.4}\text{Sr}_{0.4}\text{Zr}_{0.9}\text{Ni}_{0.1}\text{O}_{3-\delta}$ (LSZN) and $\text{La}_{0.4}\text{Sr}_{0.4}\text{Sc}_{0.9}\text{Ni}_{0.1}\text{O}_{3-\delta}$ (LSSN) were also synthesized by the identical procedure as LSTN, with the exception of the distinction of their raw materials. e-LSTN was prepared by treating LSTN in an atmosphere of 10% H_2 /90%Ar at 900°C for 10 h. The other exsolved samples, namely, e-LSTC, e-LSTF, e-LSTNF, e-LSTNC, e-LSZN and e-LSSN, were also obtained by treating their respective perovskite precursor at the same thermal treatment condition as e-LSTN. The commercial bulk Ni and nano Ni powders was purchased from Sinopharm Chemical Reagent Co. Ltd and Aladdin Industrial Corporation, respectively.

Basic characterizations. Powder X-ray diffraction (XRD) patterns were collected on a Rigaku Smartlab diffractometer with filtered $\text{Cu K}\alpha$ radiation operating at a tube voltage of 40 kV and current of 40 mA in a step-scan mode within the range of 20 - 80° . Scanning electron microscopy (SEM) images was obtained on a Hitachi S-4800 scanning electron micro-analyzer. Transmission electron microscopy (TEM) images were taken on an FEI Tecnai G2T20 electron microscope operating at 200 kV. The high-angle annular dark-field scanning transmission electron microscopy (HAADF-STEM) and the corresponding energy-dispersive X-ray spectroscopy (EDX) analysis were taken on an FEI Tecnai G2 F30 STWIN field-emission transmission electron microscope equipped with an EDX analyzer at 200

kV. The surface element states were determined by X-ray photoelectron spectroscopy (XPS, PHI5000 VersaProbe spectrometer equipped with an Al K α X-ray source) and data were fitted by the public software package XPSPEAK.

Working Electrode preparation. Working electrodes for HER and OER tests were prepared by a controlled drop-casting approach involving an RDE made of glassy carbon (GC, 0.196 cm², Pine Research Instrumentation). Before use, the GC electrodes were pre-polished using aqueous alumina suspension. To remove any electrode conductivity limitations within thin film electrodes, all the catalysts were mixed with as-received conductive carbon (Super P Li) at a mass ratio of 1:1. Briefly, the suspensions were prepared by sonication of a mixture of catalyst (10 mg), conductive carbon (10 mg), Nafion solution (5 wt%, 100 μ L), and ethanol (1 mL) for at least 1 h to generate a homogeneous ink. Next, a 5 μ L aliquot of as-prepared catalyst ink was dropped on the surface of the GC substrate, yielding an approximate catalyst loading of 0.464 mg_{total} cm⁻² (0.232 mg_{catalyst} cm⁻²) and was left to dry prior to the electrochemical tests.

Electrochemical measurements. Electrochemical HER and OER activity of catalysts in 0.1 M KOH solution were conducted at room temperature in a standard three-electrode electrochemical cell (Pine Research Instrumentation) with an RDE configuration controlled by a CHI 760D electrochemistry workstation. Catalysts cast on RDE Ag/AgCl (3.5 M KCl) were used as the working electrode and reference electrode, respectively. Graphite rod for HER tests and Pt foil for OER tests were used as the counter electrodes, respectively. During each electrochemical measurement, RDE electrode was constantly rotating at 1600 rpm to remove the bubbles. The electrolyte was bubbled with Ar or O₂ for ~30 min prior to HER or OER tests and maintained under Ar or O₂ atmosphere throughout the test period. HER polarization curves obtained from linear sweep voltammetry (LSVs) was recorded at a scan rate of 5 mV s⁻¹ from -0.8 to -1.6 V vs. Ag/AgCl and OER polarization curves was recorded from 0.2 to 1 V vs. Ag/AgCl. All polarization curves were *iR* corrected in this study unless noted otherwise. The polarization curves were replotted as overpotential versus the logarithm of current density (log|*j*|) to obtain Tafel plots. Electrochemical impedance spectra (EIS) were performed from 10 kHz to 0.1 Hz at -1.3 V vs. Ag/AgCl under the influence of an AC voltage of 10 mV. Cycle voltammetry (CV) method was used to measure the electrochemical double layer capacitance (C_{dl}). The potential was swept at different scan rates of 20, 40, 60, 80 and 100 mV s⁻¹ from -0.8 to -0.9 V vs. Ag/AgCl, where no faradic current was observed. The halves of the positive and negative current density differences at the center of the scanning potential range (i.e., -0.85 V) were plotted versus scan rates where the slopes represent the double layer capacitance.

II. Supplementary Results

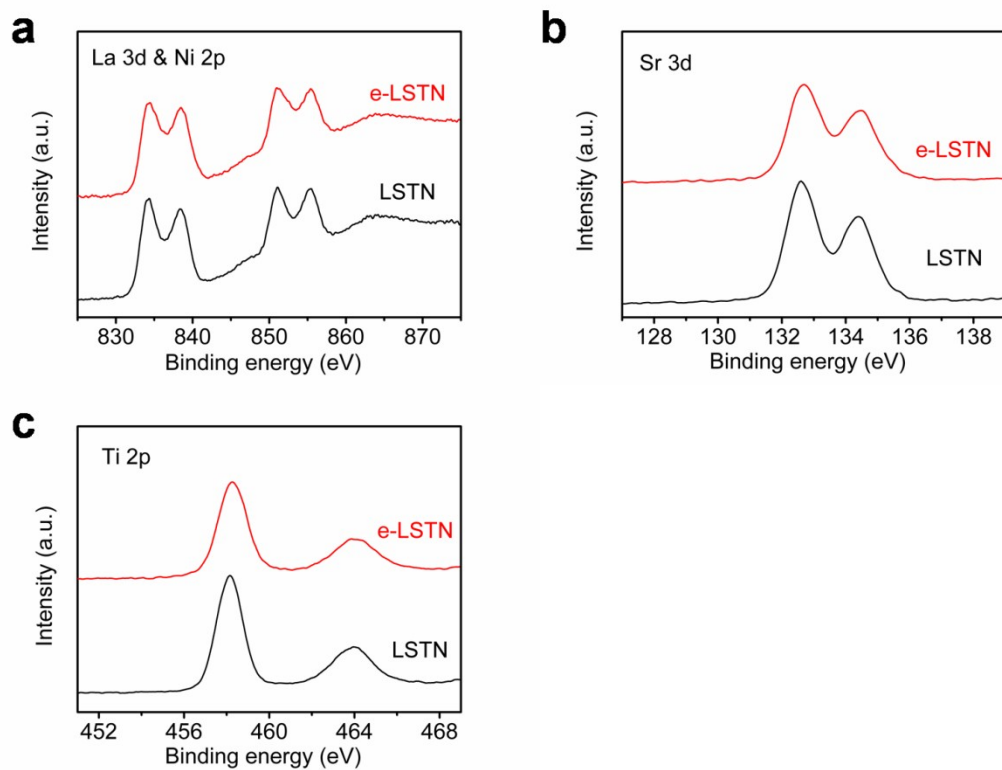


Fig. S1. XPS spectra of (a) La 3d & Ni 2p, (b) Sr 3d, and (c) Ti 2p for LSTN and e-LSTN.

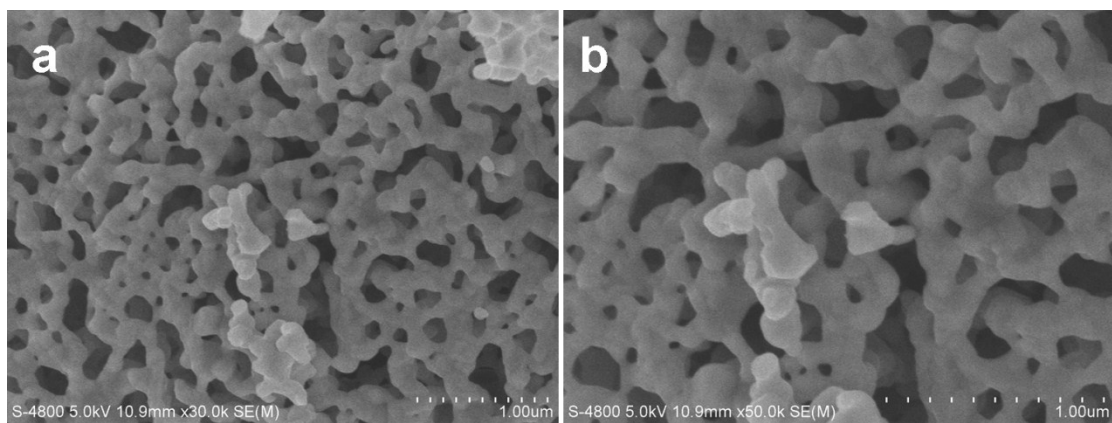


Fig. S2. SEM images with different magnifications of LSTN.

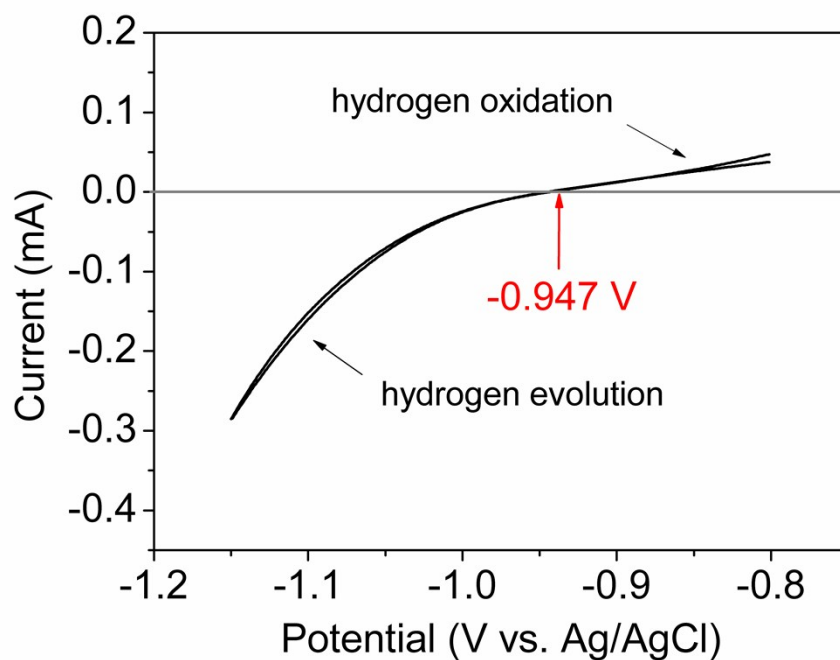


Fig. S3. Potential calibration of the Ag/AgCl reference electrode in 0.1 M KOH solution. The calibration was performed in a high purity hydrogen-saturated electrolyte with a platinum rotating disk electrode (PINE, 4 mm diameter, 0.126 cm²) as the working electrode. Cyclic voltammetry (CV) was run at a scan rate of 1 mV s⁻¹, and the average of the two potentials at which the current crossed zero was taken to be the thermodynamic potential for the hydrogen electrode reaction. In 0.1 M KOH, $E_{\text{RHE}} = E_{\text{Ag/AgCl}} + 0.947 \text{ V}$.

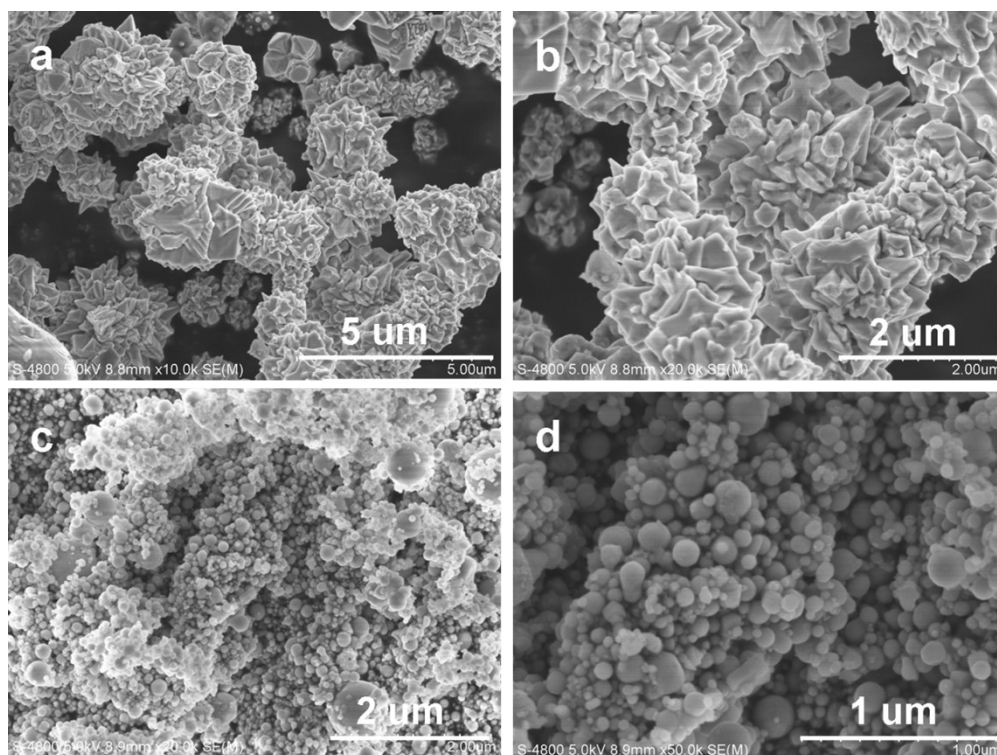


Fig. S4. SEM images of commercial (a,b) bulk Ni (Sinopharm Chemical Reagent Co. Ltd) and (c,d) nano Ni (Aladdin Industrial Corporation) powders.

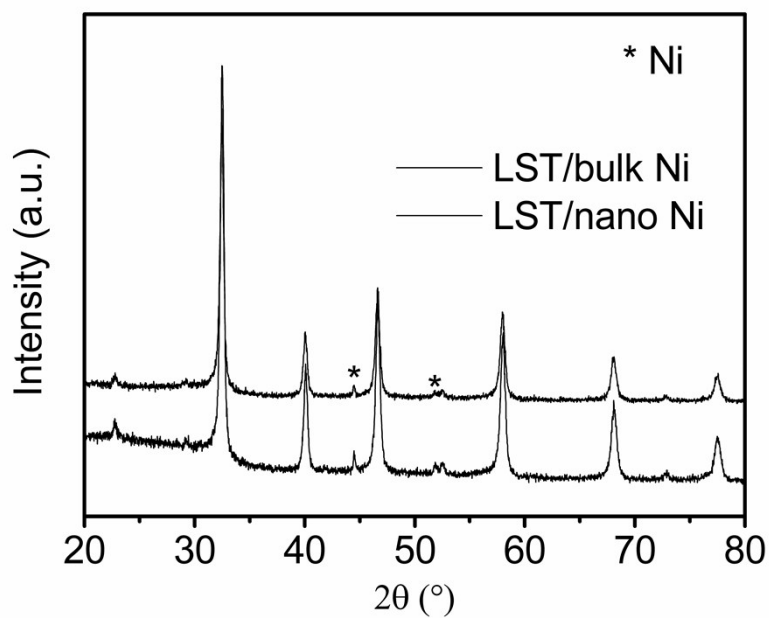


Fig. S5. XRD patterns of LST/bulk Ni and LST/nano Ni samples by physical mixing.

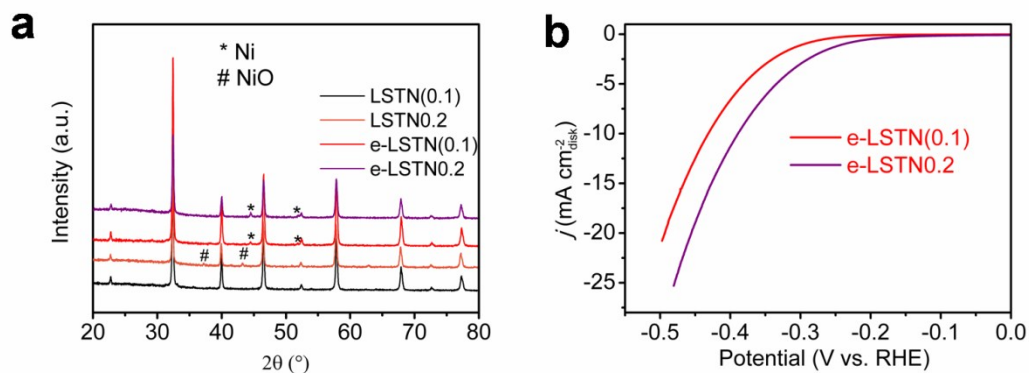


Fig. S6. (a) XRD patterns of LSTN(0.1), LSTN0.2, e-LSTN(0.1) and e-LSTN0.2 powders. With further increase in Ni content to 6.24 wt% in the $\text{La}_{0.4}\text{Sr}_{0.4}\text{Ti}_{0.8}\text{Ni}_{0.2}\text{O}_{3-\delta}$, small quantities of NiO phase emerges, suggesting that the limit of Ni solubility in the Ti site of LST perovskite is around 20%. (b) Polarization curves of e-LSTN(0.1) and e-LSTN0.2 catalysts in an Ar-saturated 0.1 M KOH solution.

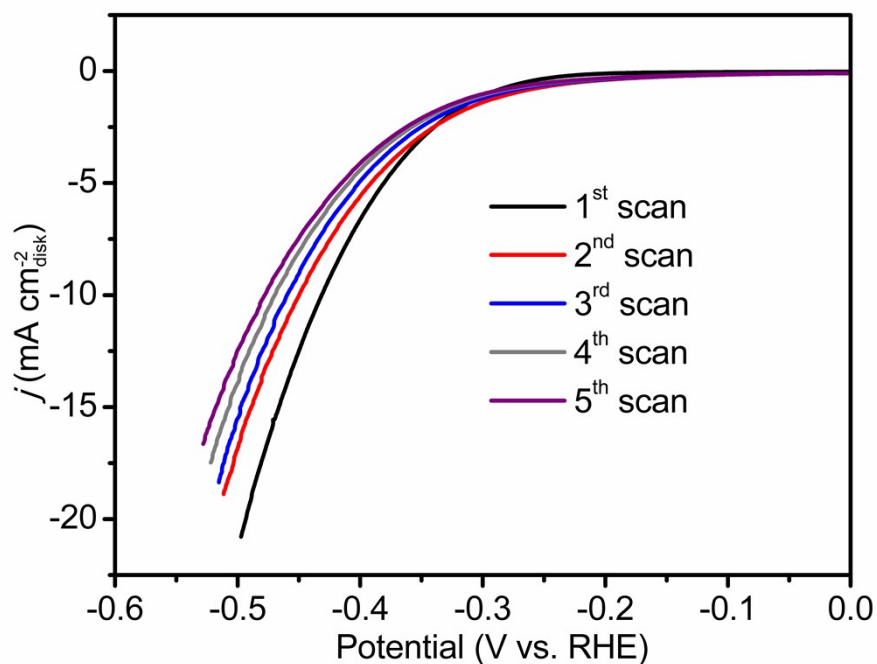


Fig. S7. Short-term stability test with the first five LSV scans for e-LSTN catalyst.

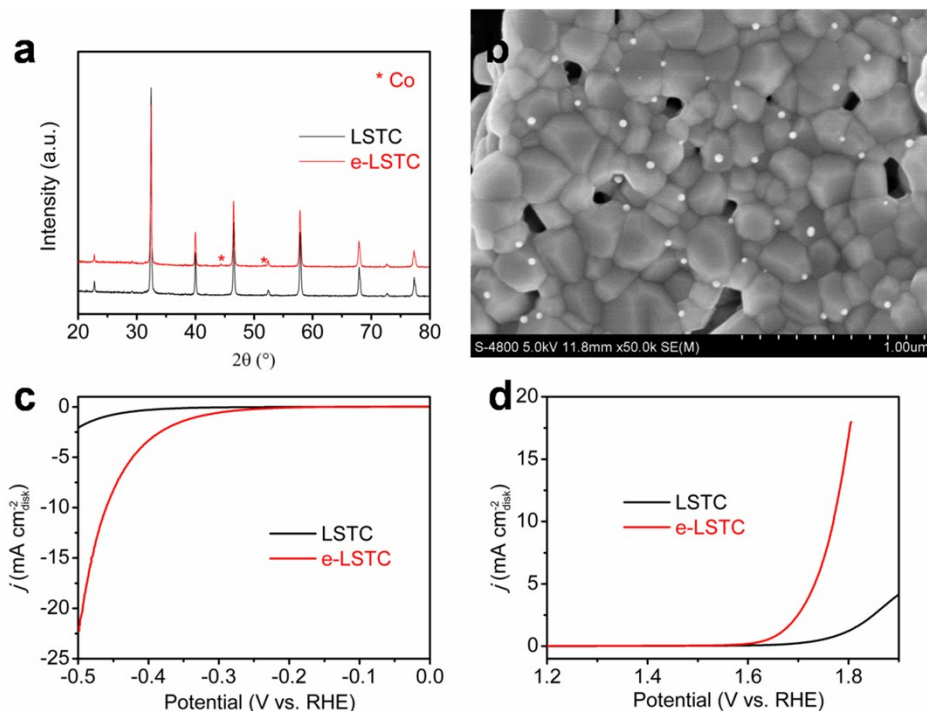


Fig. S8. (a) XRD patterns of LSTC and e-LSTC. (b) SEM image of e-LSTC. (c) HER polarization curves of LSTC and e-LSTC catalysts in an Ar-saturated 0.1 M KOH solution. (d) OER polarization curves of LSTC and e-LSTC catalysts in an O₂-saturated 0.1 M KOH solution.

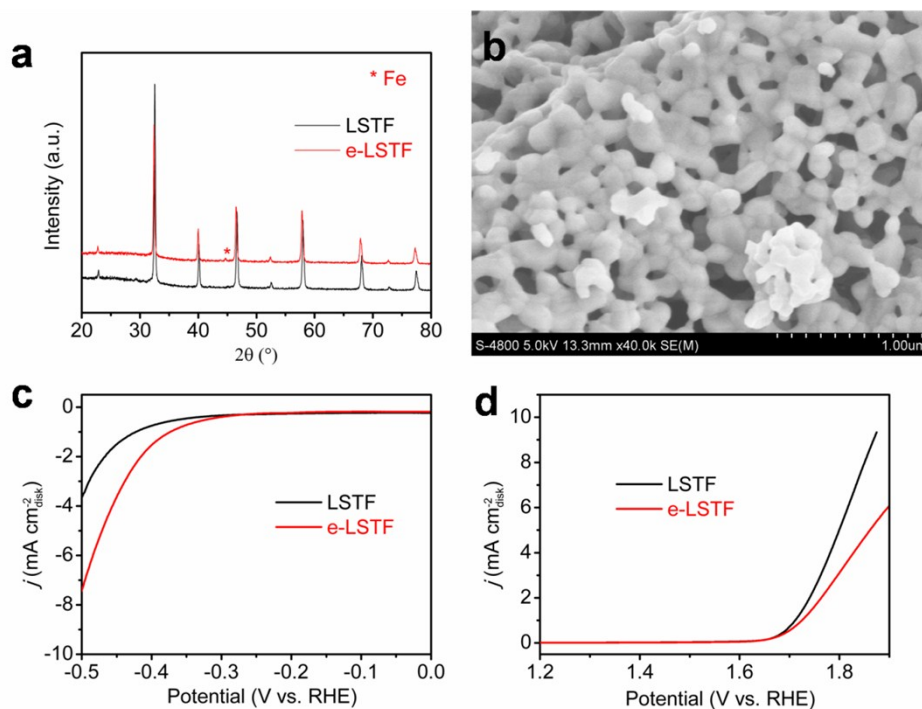


Fig. S9. (a) XRD patterns of LSTF and e-LSTF. (b) SEM image of e-LSTF. (c) HER polarization curves of LSTF and e-LSTF catalysts in an Ar-saturated 0.1 M KOH solution. (d) OER polarization curves of LSTF and e-LSTF catalysts in an O₂-saturated 0.1 M KOH solution.

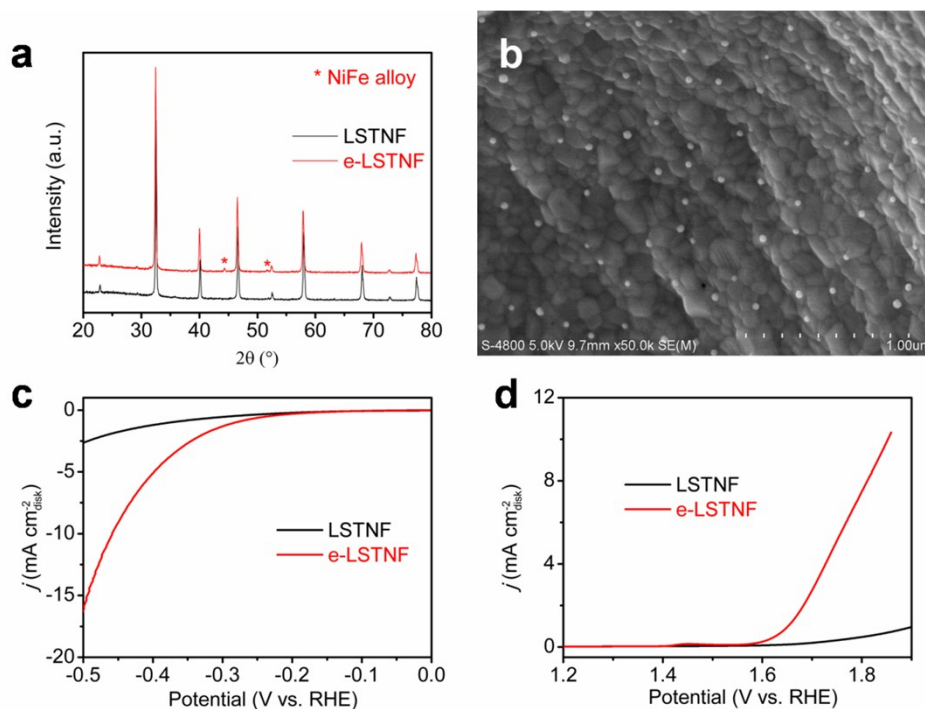


Fig. S10. (a) XRD patterns of LSTNF and e-LSTNF. (b) SEM image of e-LSTNF. (c) HER polarization curves of LSTNF and e-LSTNF catalysts in an Ar-saturated 0.1 M KOH solution. (d) OER polarization curves of LSTNF and e-LSTNF catalysts in an O₂-saturated 0.1 M KOH solution.

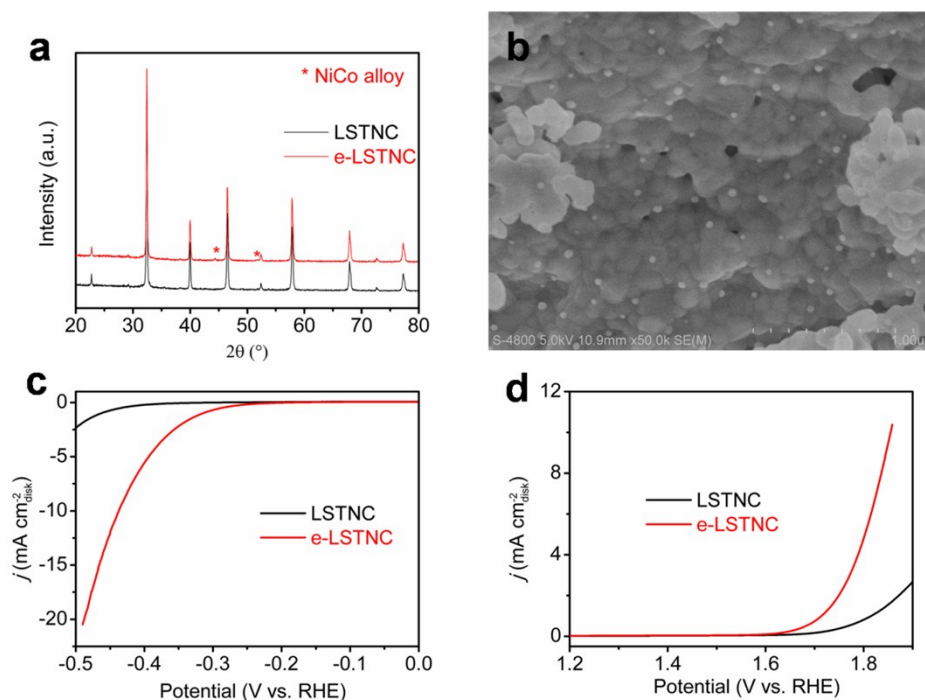


Fig. S11. (a) XRD patterns of LSTNC and e-LSTNC. (b) SEM image of e-LSTNC. (c) HER polarization curves of LSTNC and e-LSTNC catalysts in an Ar-saturated 0.1 M KOH solution.

(d) OER polarization curves of LSTNC and e-LSTNC catalysts in an O₂-saturated 0.1 M KOH solution.

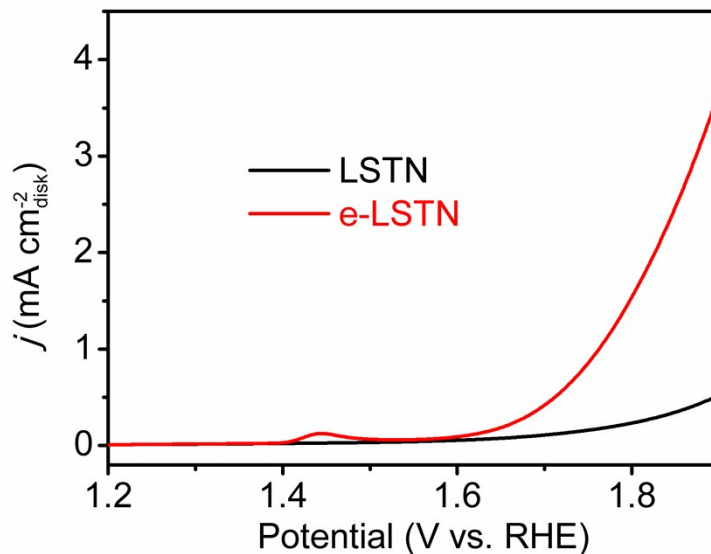


Fig. S12. OER polarization curves of LSTN and e-LSTN catalysts in an O₂-saturated 0.1 M KOH solution.

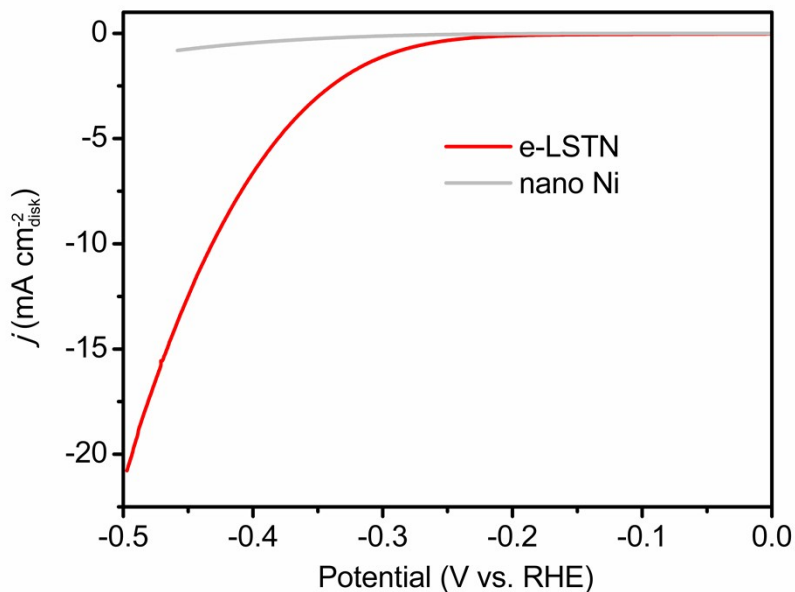


Fig. S13. HER polarization curves of e-LSTN and nano Ni catalysts in an Ar-saturated 0.1 M KOH solution. The carbon supported e-LSTN and Ni nanoparticles have identical Ni mass loading of 0.00724 mg cm⁻² on the RDE.

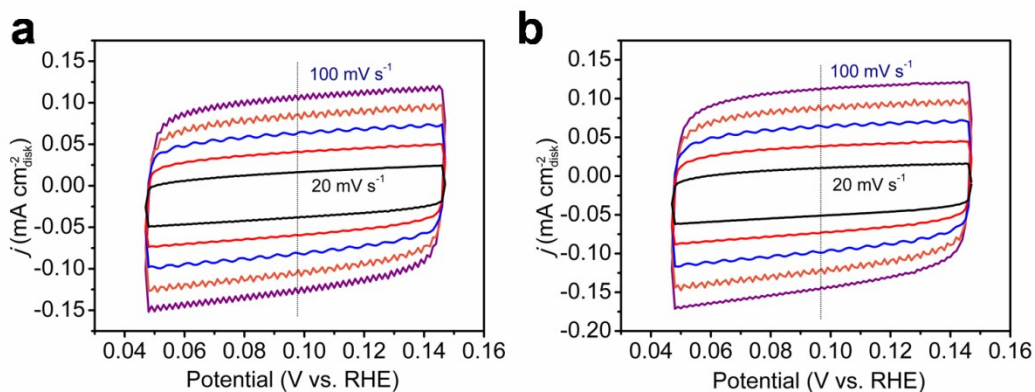


Fig. S14. CV measurements in a non-faradic current region (0.047-0.147 V vs. RHE, no iR -corrected) at scan rates of 20, 40, 60, 80 and 100 mV s⁻¹ of (a) LSTN and (b) e-LSTN catalysts in 0.1 M KOH solution.

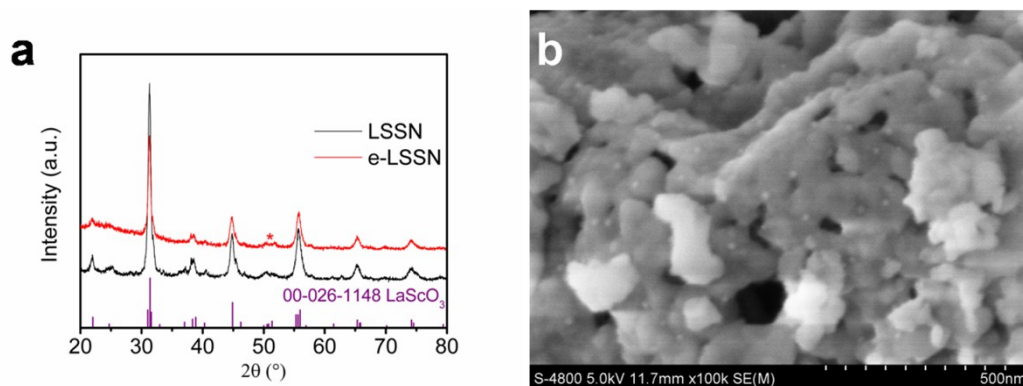


Fig. S15. (a) XRD patterns of LSSN and e-LSSN. * marks the part peak of exsolved Ni in e-LSSN. (b) SEM image of e-LSSN.

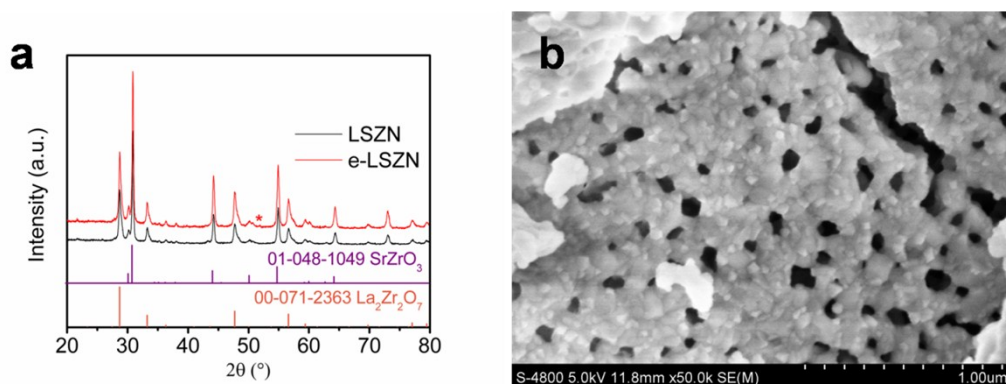


Fig. S16. (a) XRD patterns of LSZN and e-LSZN. * marks the part peak of exsolved Ni in e-LSZN. Besides, the as-synthesized LSZN is the mixture perovskite phases of SrZrO₃ and La₂Zr₂O₇, but two phases both contains Zr⁴⁺. (b) SEM image of e-LSZN.

Table S1. O 1s XPS peak deconvolution results.

Electrocatalysts	lattice O ²⁻	O ₂ ^{2-/O} -	-OH	H ₂ O or CO ₃ ²⁻
LSTN	53.7%	30.2%	10.8%	5.3%
e-LSTN	53.6%	27.6%	13.1%	5.7%

O 1s XPS spectra can be deconvoluted into four different characteristic peaks, i.e., lattice oxygen species (~529.2 eV for O²⁻), highly oxidative oxygen species (~530.0 eV for O₂^{2-/O}-), hydroxyl groups or the surface adsorbed oxygen (~531.3 eV for -OH), and adsorbed molecular water or carbonates (~532.4 eV for H₂O or CO₃²⁻)^[S2-S7]. The content of surface -OH in e-LSTN is slightly higher than that of LSTN.

Reference

- [S1] Z. Shao, S. Haile. *Nature* 2004, **431**, 170.
[S2] Y. G. Wang, J. W. Ren, Y. Q. Wang, F. Y. Zhang, X. H. Liu, Y. Guo, G. Z. Lu, *J. Phys. Chem. C* 2008, **112**, 15293.
[S3] R. C. Liu, F. L. Liang, W. Zhou, Y. S. Yang, Z. H. Zhu, *Nano Energy* 2015, **12**, 115.
[S4] Y. L. Zhu, W. Zhou, J. Yu, Y. B. Chen, M. L. Liu, Z. P. Shao, *Chem. Mater.* 2016, **28**, 1691.
[S5] F. L. Liang, Y. Yu, W. Zhou, X. Y. Xu, Z. H. Zhu, *J. Mater. Chem. A*. 2015, **3**, 634.
[S6] X. M. Xu, Y. B. Chen, W. Zhou, Z. H. Zhu, C. Su, M. L. Liu, Z. P. Shao, *Adv. Mater.* 2016, **28**, 6442.
[S7] W. Zhou, M. W. Zhao, F. L. Liang, S. C. Smith, Z. H. Zhu, *Mater. Horiz.* 2015, **2**, 495.